Journal of Alloys and Compounds 508 (2010) 582–586

Contents lists available at ScienceDirect

Journal of Alloys and Compounds

journal homepage: www.elsevier.com/locate/jallcom

Effect of boron-doping on thermoelectric properties of rutile-type titanium dioxide sintered materials

Hiroyuki Kitagawa*, Toshimitsu Kunisada, Yasuji Yamada, Shugo Kubo

Department of Materials Science, Shimane University, 1060 Nishikawatsu, Matsue, Shimane 690-8504, Japan

ARTICLE INFO

Article history:
Received 16 June 2010
Received in revised form 24 August 2010
Accepted 25 August 2010
Available online 28 September 2010

Keywords:
Titanium oxide
Sintering
Boron-doping
Thermoelectric properties

ABSTRACT

The electrical and thermal transport properties of boron-doped rutile-type TiO_2 were investigated. The rutile-type TiO_2 powder was mixed with B_2O_3, TiB_2 or B and the mixtures were sintered using the pulse current sintering method at 1473 K. Secondary ion mass spectroscopy (SIMS) and X-ray diffraction (XRD) measurements showed that B or TiB_2 addition was effective for boron-doping. The boron was well distributed in the sintered materials and the unit cell volume of rutile increased as the amounts of added B or TiB_2 increased. The electrical resistivity and Seebeck coefficient at 300 K decreased with an increase in the unit cell volume indicating that boron addition leads to an increase in the electron concentration. Thermal conductivity at room temperature also decreased with an increase in unit cell volume and as a result the thermoelectric figure of merit for rutile-type TiO_2 was enhanced by boron-doping.

1. Introduction

Titanium dioxide (TiO_2) is used in a wide range of applications because of its excellent cost performance, chemical stability, non-toxicity and controllable semiconducting properties [1]. TiO_2 has been found to be an insulator when the crystal structure is perfectly formed; however, the electrical properties of TiO_2 can be controlled by oxygen vacancies [2,3] and by impurity doping. It is well known that niobium doping is effective in enhancing the electrical conductivity of TiO_2 [1,4–7]. Other elements such as Fe [8], Ni [9], Pd and V [10], and Cr [11] have been used for doping to control the electrical properties of TiO_2. Moreover, doping with non-metallic elements such as N [12], F [13,14] and B [15,16] has been also examined to improve the photocatalytic properties of TiO_2.

For thermoelectric applications, the increase in electrical conductivity has been attempted by reduction treatment of rutile-type bulks [17] and Nb-doping for anatase-type thin films [18]. These are effective for controlling the thermoelectric properties. However, the thermoelectric properties of TiO_2 doped with non-metallic elements have not been investigated. Thus, it is necessary to understand the effects of non-metallic elements on the electrical and thermal transport properties of TiO_2. This understanding may allow the development of TiO_2-based materials with controlled thermoelectric properties.

This study focused on the effects of boron-doping on the structure and thermoelectric properties of rutile-type TiO_2 (RTO). Boron-doping was performed by mixing B_2O_3, TiB_2 and B with RTO powder and pulse current sintering. Structural properties were identified by X-ray diffraction (XRD) and secondary ion mass spectroscopy (SIMS). Electrical resistivity, Hall and Seebeck coefficients, and thermal conductivity were measured to evaluate the thermoelectric properties.

2. Experimental

Boron-doped RTO was prepared by pulse current sintering. A RTO powder was used as the starting material and B_2O_3, TiB_2 and B powders were selected as a boron source. These materials were weighed and mixed to give nominal compositions of TiO_2–x mol% B_2O_3 (x = 1, 5), TiB_2 (x = 0.5, 1) and B (x = 1, 5). Each mixture was placed in a graphite die and a mechanical pressure of 40 MPa was applied through graphite punches. The mixture was heated to 1473K by applying a pulse current. After 10 min at this temperature, the material was allowed to cool naturally to room temperature. The undoped RTO was also prepared by the above-mentioned method. The resultant sintered materials were 5 mm in thickness and 10 mm in diameter and the density was higher than 96% of the theoretical density of RTO.

The phase constitution and lattice parameters of the prepared materials were determined by X-ray diffraction using Cu-Kα radiation. Boron concentration profiles were qualitatively determined by secondary ion mass spectrometry (SIMS), where O^{2+} ions (5 keV, 500 nA) were used as the primary ion beam. Hall coefficients R_H and electrical resistivity ρ were measured by the van der Pauw method from 30 to 300 K. Seebeck coefficient S was measured by applying a temperature difference ΔT of 1–3 K at 300 K. Thermal diffusivity α was measured by the laser flash method at room temperature and the thermal conductivity κ was calculated using the following standard expression: $\kappa = \alpha \cdot C_P \cdot D$, where D is the bulk density measured by the Archimedes method and C_P is the specific heat of RTO [19]. Thermoelectric properties were evaluated by the figure of merit $Z = S^2/\rho\kappa$.

* Corresponding author. Tel.: +81 852 32 6076; fax: +81 852 32 6409.
E-mail address: kitagawa@riko.shimane-u.ac.jp (H. Kitagawa).

0925-8388/$ – see front matter © 2010 Elsevier B.V. All rights reserved.
doi:10.1016/j.jallcom.2010.08.125

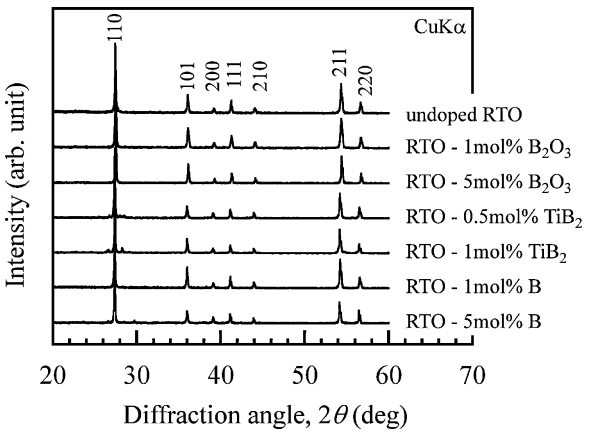

Fig. 1. X-ray diffraction patterns of undoped and boron-doped RTO.

3. Results and discussion

3.1. Structures

Fig. 1 shows the X-ray diffraction patterns of the prepared sintered materials. The rutile-type structure was predominant in RTO–x mol% B_2O_3 (x = 1, 5), TiB_2 (x = 0.5, 1) and B (x = 1, 5). Other titanium oxide phases such as Ti_3O_5, Ti_4O_7 and Ti_5O_9 appeared when doping with B or TiB_2 was heavy (*e.g.* RTO–10 mol% B and RTO–5 mol% TiB_2).

From these XRD patterns, the lattice parameter of RTO was calculated and plotted in terms of the nominal concentration of additives as shown in Fig. 2(a) and (b) for the a- and c-axes, respectively. In the case of B and TiB_2 addition, a- and c-axes lattice parameters tended to increase as the nominal concentration of additives was increased. As a result, the unit cell volume increased with an increase in the nominal concentration of additives as shown in Fig. 2(c). Lu et al. reported that the distance between crystal planes decreased after the introduction of oxygen vacancies into RTO [17]. Therefore, the increase in unit cell volume is attributed to the introduction of boron into RTO. On the other hand, lattice parameters and unit cell volume were almost constant for B_2O_3 addition. This result might be due to the vaporization of B_2O_3 during the sintering process because of its low melting point. Therefore, B_2O_3 is not effective for the boron-doping of RTO.

Fig. 3(a) shows the SIMS results for RTO–1 mol% B_2O_3, RTO–1 mol% TiB_2 and RTO–5 mol% B where the intensity of the ^{11}B signals were normalized by the intensity of ^{50}Ti and plotted in terms of depth from the surface of the sintered materials. The secondary ion signal of boron was detected in all samples and no positional dependence was found in the measured area. It is noteworthy that the RTO with uniform distribution of boron could be prepared by a short time process. This result suggests the large diffusion rate of boron. The interstitial diffusion may occur in the case of elements of small atomic radius such as boron and the interstitial diffusion is extremely rapid as compared with the vacancy diffusion. The intensity ratio was large for 5 mol% B and 1 mol% TiB_2 addition samples and small in the 1 mol% B_2O_3 addition sample.

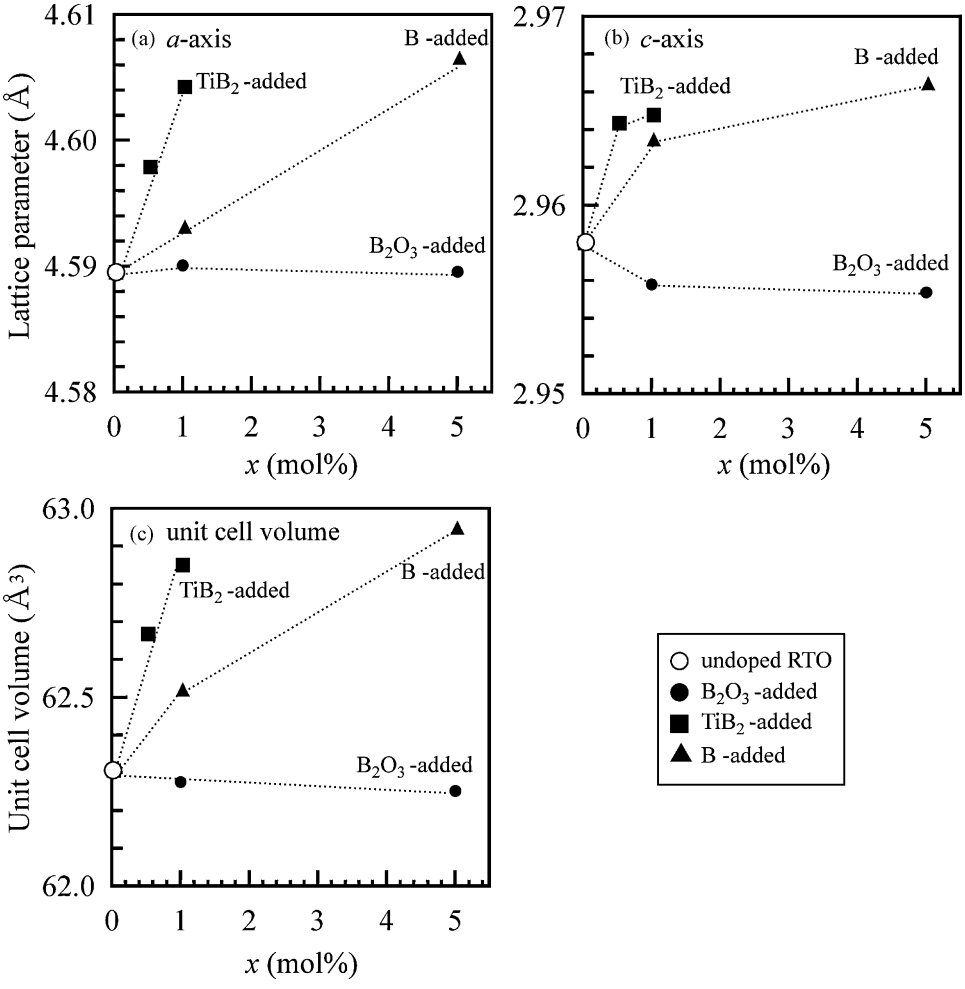

Fig. 2. Lattice parameters of undoped and boron-doped RTO. (a) a-axis, (b) c-axis and (c) unit cell volume plotted in terms of nominal additive concentrations.

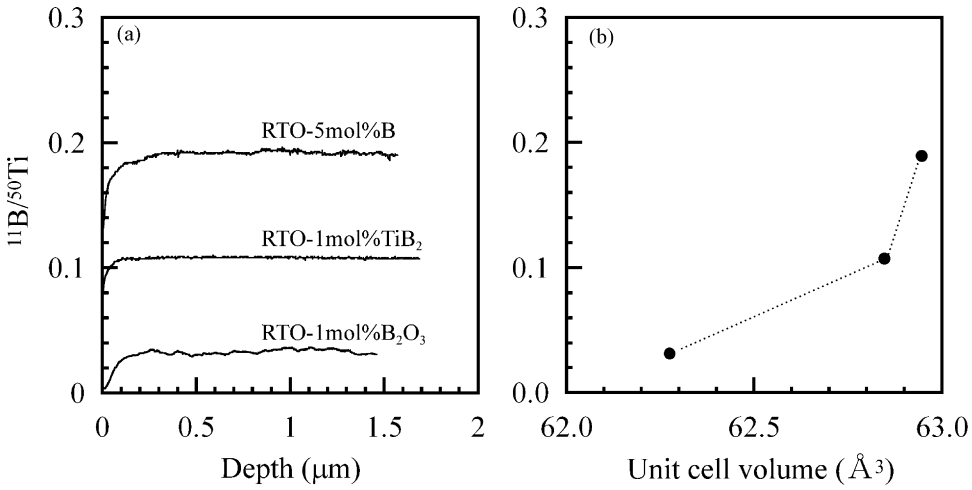

Fig. 3. SIMS results of RTO–1 mol% B_2O_3, RTO–1 mol% TiB_2 and RTO–5 mol% B. $^{11}B/^{50}Ti$ was plotted in terms of (a) depth from the surface of sintered materials and (b) unit cell volume.

This tendency is related to a change in unit cell volume. Therefore, we plotted $^{11}B/^{50}Ti$ as a function of the unit cell volume as shown in Fig. 3(b). A good relationship between boron concentration and unit cell volume is evident. Therefore, we conclude that the introduction of boron increases the unit cell volume and boron-doping of RTO can be achieved by a powder-metallurgical method with the correct additive.

3.2. Thermoelectric properties

The Hall and Seebeck coefficients of all sintered materials were negative, indicating that the majority carriers are electrons. Fig. 4 shows the electrical resistivity at 300 K for undoped and boron-doped RTO plotted in terms of the unit cell volume. The resistivity tends to decrease with an increase in the unit cell volume. The electron carrier concentration at 300 K, estimated by the measured Hall coefficient, was 7.5×10^{25} m^{-3}, 5.6×10^{26} m^{-3} and 2.1×10^{26} m^{-3} for undoped, RTO–0.5 mol% TiB_2 and RTO1– mol% B, respectively. These results strongly suggest that the boron is a donor-like impurity in RTO because the increase in unit cell volume should correspond to the increase in boron content.

The temperature dependence of the electrical resistivity of undoped, RTO–5 mol% B, RTO–1 mol% TiB_2 and RTO–1 mol% B_2O_3 is shown in Fig. 5. The plots are in the Arrhenius style and the activation energy (E_a) was determined from the slope using the relationship, $\rho \propto \exp(E_a/kT)$. The electrical resistivity of all the samples decreased with an increase in temperature, which is typical semiconductor behavior. The activation energy in the low temperature range (30–100 K) was approximately 20 meV for both the undoped and boron-doped samples. This shows that oxygen vacancies, which may have been introduced during sintering, were the main carrier (electrons) source at low temperature. In the high temperature region, the activation energy of RTO–5 mol% B and RTO–1 mol% TiB_2 was large at approximately 50 meV. Undoped RTO and RTO–1 mol% B_2O_3, which had a low boron concentration, had an activation energy of 20 meV.

From this fact, we deduce the two mechanisms of the boron-doping effect. Mechanism one is the change of the oxygen vacancy number by boron-doping. Breckenridge and Hosler reported that there are two sources of conduction electrons in the reduced RTO [20]. The one source has a very small activation energy and ionized even at low temperatures. The other source has a comparatively large activation energy and ionized at temperatures above 150 K. As a result, the electron concentration gradually increases at low temperature and rapidly increases at temperatures above 150 K.

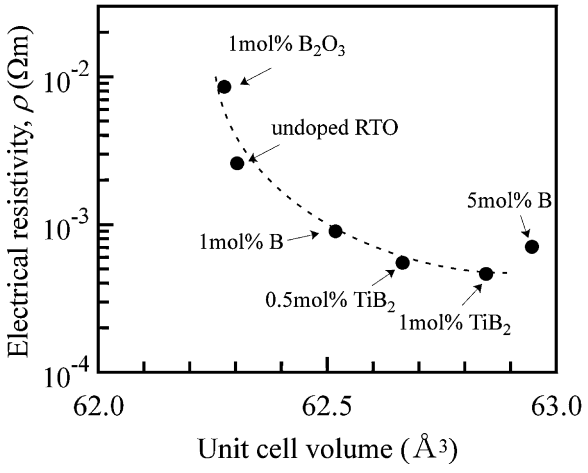

Fig. 4. Electrical resistivity at 300 K for undoped and boron-doped RTO plotted in terms of the unit cell volume.

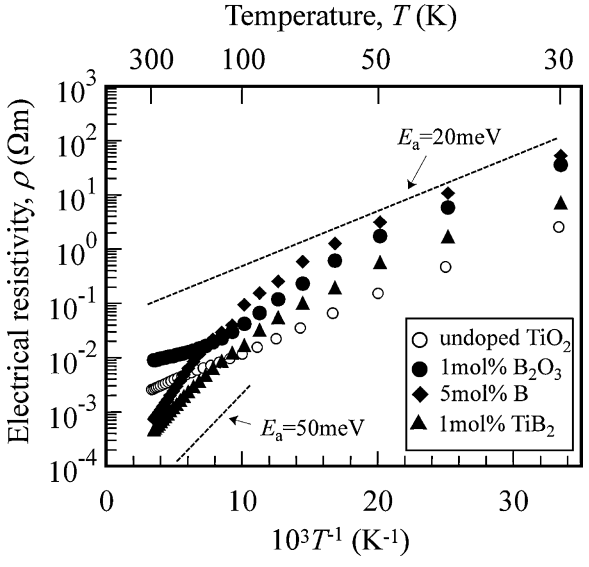

Fig. 5. Temperature dependence of the electrical resistivity of undoped, RTO–1 mol% B_2O_3, RTO–1 mol% TiB_2 and RTO–5 mol% B.

Table 1
Thermoelectric properties at 300 K of undoped and boron-doped RTO.

Nominal composition	Seebeck coefficient S (μV/K)	Electrical resistivity ρ (10^{-4} Ωm)	Thermal conductivity[a] κ (W/mK)	Figure of merit Z (10^{-5} K^{-1})
Undoped RTO	462	26.0	6.3	1.3
RTO–1 mol% B_2O_3	540	85.5	7.0	0.5
RTO–0.5 mol% TiB_2	362	5.5	4.6	5.2
RTO–1 mol% TiB_2	298	4.7	5.1	3.7
RTO–1 mol% B	436	9.0	5.7	3.7
RTO–5 mol% B	239	7.1	3.7	2.2

[a] Value at room temperature.

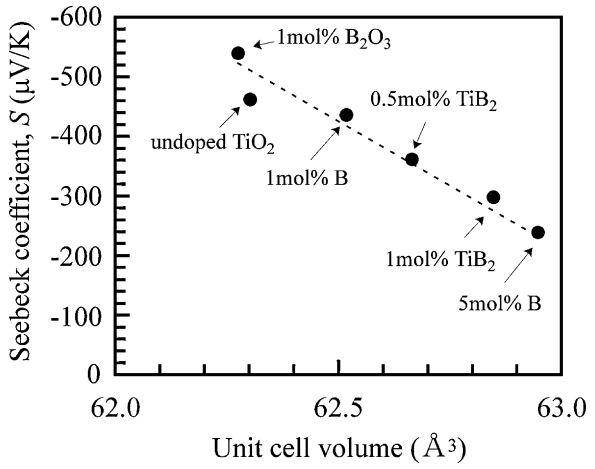

Fig. 6. Seebeck coefficient at 300 K for undoped and boron-doped RTO plotted in terms of the unit cell volume.

This temperature dependence is similar to the change of electrical resistivity for RTO–5 mol% B and RTO–1 mol% TiB_2. Mechanism two is that the ionized boron acts as a donor. That is, the doped boron forms a deep impurity level when compared with the oxygen vacancies with small activation energy. The doped boron was ionized at temperatures above 100 K and thus supplied the conduction electrons. This should lead to a rapid decrease of electrical resistivity above 100 K and a small electrical resistivity near room temperature.

Fig. 6 shows the Seebeck coefficient at 300 K for undoped and boron-doped RTO plotted in terms of the unit cell volume. The absolute value of the Seebeck coefficient $|S|$ decreased as the unit cell volume increased. This tendency is attributed to the increase in carrier concentration and is consistent with the change in the electrical resistivity. Fig. 7 shows the thermal conductivity at room temperature for undoped and boron-doped RTO and is plotted in terms of the unit cell volume. The thermal conductivity decreases as the unit cell volume increases. According to calculations based on the Wiedemann–Franz law, the lattice contribution to the thermal conductivity is predominant in all samples. These results therefore suggest that the scattering of phonons is enhanced by the added boron atoms.

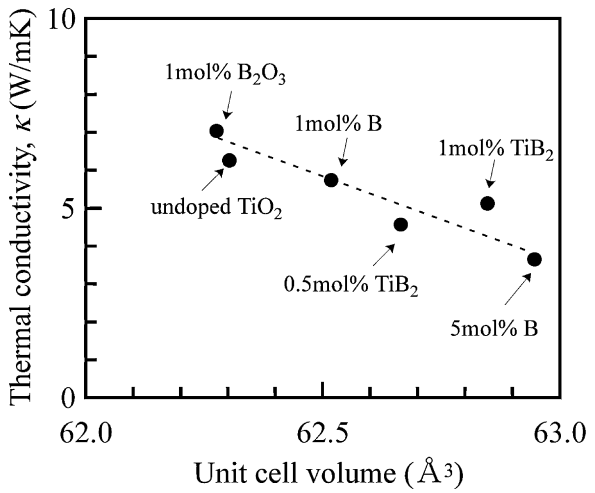

Fig. 7. Thermal conductivity at room temperature for undoped and boron-doped RTO plotted in terms of the unit cell volume.

The thermoelectric properties at 300 K for the undoped and boron-doped RTO are summarized in Table 1, where the thermal conductivity is the value at room temperature. The thermoelectric figure of merit becomes large after B or TiB_2 addition because boron acts as a donor impurity as well as a phonon scattering center. We conclude that the electrical and thermal transport properties of RTO are controllable by boron-doping and the thermoelectric figure of merit can be improved using B or TiB_2 as additives.

4. Conclusions

Boron-doped rutile-type TiO_2 was prepared by pulsed current sintering. Structural analyses showed that B or TiB_2 addition was effective for boron-doping and B_2O_3 addition was not effective. The electrical resistivity and the thermal conductivity decreased after the addition of B or TiB_2 indicating that boron acts as an electron carrier source and a phonon scattering center. As a result, the thermoelectric figure of merit is enhanced by boron-doping. The maximum figure of merit obtained in this study was 5.2×10^{-5} K^{-1} at 300 K for RTO–0.5 mol% TiB_2. This value is four times larger than the value for undoped RTO.

Acknowledgments

Thermal diffusivity measurements were obtained with support from the Research Institute for Sustainable Humanosphere (RISH) at Kyoto University as a collaborative research project. The authors are grateful to Dr. T. Hata and Dr. J. Sulistyo for their experimental assistance.

References

[1] F.A. Grant, Rev. Mod. Phys. 31 (1959) 646.
[2] M.K. Nowotny, T. Bak, J. Nowotny, J. Phys. Chem. B 110 (2006) 16270.
[3] J. Tang, W. Wang, G.L. Zhao, Q. Li, J. Phys.: Condens. Matter 21 (2009) 205703.
[4] Y. Funabayashi, T. Hitosugi, Y. Yamamoto, Y. Hirose, G. Kinoda, K. Inada, T. Shimada, T. Hasegawa, Thin Solid Films 496 (2006) 157.
[5] N. Yamada, T. Hotosugi, N.L.H. Hoang, Y. Funabayashi, Y. Hirose, T. Shimada, T. Hasegawa, Jpn. J. Appl. Phys. 46 (2007) 5275.
[6] N. Yamada, T. Hitosugi, N.L.H. Hoang, Y. Funabayashi, Y. Hirose, S. Konuma, T. Shimada, T. Hasegawa, Thin Solid Films 516 (2008) 5754.
[7] L.R. Sheppard, T. Bak, J. Nowotny, M.K. Nowotny, Int. J. Hydrogen Energy 32 (2007) 2660.
[8] A.R. Bally, E.N. Korobeinikova, P.E. Schmid, F. Lévy, F. Bussy, J. Phys. D 31 (1998) 1149.
[9] F. Yakuphanoglu, M. Okutan, K. Korkmaz, J. Alloy Compd. 450 (2008) 39.
[10] J. Domaradzki, Thin Solid Films 497 (2006) 243.
[11] D. Mardare, G.I. Rusu, F. Iacomi, M. Girtan, I.V. Simiti, Mater. Sci. Eng. B 118 (2005) 187.
[12] M. Batzill, E.H. Morales, U. Diebold, Phys. Rev. Lett. 96 (2006) 026103.

[13] D. Li, H. Haneda, S. Hishita, N. Ohashi, N.K. Labhsetwar, J. Fluorine Chem. 126 (2005) 69.
[14] N. Todorova, T. Giannakopoulou, T. Vaimakis, C. Trapalis, Mater. Sci. Eng. B 152 (2008) 50.
[15] Y. Su, S. Han, X. Zhang, X. Chen, L. Lei, Mater. Chem. Phys. 110 (2008) 239.
[16] V. Gombac, L. De Rogatis, A. Gasparotto, G. Vicario, T. Montini, D. Barreca, G. Balducci, P. Fornasiero, E. Tondello, M. Graziani, Chem. Phys. 339 (2007) 111.
[17] Y. Lu, M. Hirohashi, K. Sato, Mater. Trans. 47 (2006) 1449.
[18] D. Kurita, S. Ohta, K. Sugiura, H. Ohta, K. Koumoto, J. Appl. Phys. 100 (2006) 096105.
[19] S.J. Smith, R. Stevens, S. Liu, G. Li, A. Navrotsky, J. Boerio-Goates, B.F. Woodfield, Am. Mineral. 94 (2009) 236.
[20] R.G. Breckenridge, W.R. Hosler, Phys. Rev. 91 (1953) 793.